

Electronic Supplementary Information for:

Effects of Acid-alkaline Environment on the Reactivity of the 5-Carboxycytosine with Hydroxyl Radical

Lingxia Jin^{*,a} Caibin Zhao^a Tianlei Zhang^a Zhiyin Wang^a Suotian Min^a

Wenliang Wang^{*,b} Yawen Wei^c

^a *Shaanxi Province Key Laboratory of Catalytic Fundamentals & Applications, School of Chemical & Environment Science, Shaanxi University of Technology, Hanzhong, Shaanxi 723001*

^b *Key Laboratory for Macromolecular Science of Shaanxi Province, School of Chemistry and Chemical Engineering, Shaanxi Normal University, Xi'an 710062*

^c *Institute of publication Science, Chang'an University, Xi'an 710064*

* Corresponding authors. Tel: +86-916-2641660; e-mail: jinx@snut.edu.cn (L.X. Jin) ; Tel: +86-29-81530815 Fax: +86-29-81530727; e-mail: wlwang@snnu.edu.cn (W. L. Wang).

Table contents:

Table S1 Relative Energies (in $\text{kJ}\cdot\text{mol}^{-1}$) of Different Protonated 5-caCyt Isomers Both in the Gas and Aqueous Phases

Table S2 The Comparison of the Activation Free Energies (in $\text{kJ}\cdot\text{mol}^{-1}$) by G3B3 and CB3-QB3 Composite Approaches

Table S3 Spin Contamination ($\langle S^2 \rangle$) and After Spin Annihilation ($\langle S_a^2 \rangle$) Values in $\bullet\text{OH}$ -mediated 5-caCyt, 5-caCytN3⁺ and 5-CytCOO⁻ Reactions

Table S4 The Relevant Energy Information (in $\text{kJ}\cdot\text{mol}^{-1}$) of Different 5-caCyt Isomers Both in the Gas and Aqueous Phases

Table S5 The Energy Information for the Addition of $\bullet\text{OH}$ to C2, N3, C4, C7 Sites of 5-caCyt Both in the Gas and Aqueous Phases

Table S6 The Nucleus-independent Chemical Shifts (NICS(0)) for the Product Radicals of $\bullet\text{OH}$ Abstraction from 5-caCyt in the Gas Phase

Table S7 The Energy Information for the Addition of $\bullet\text{OH}$ to C2, C4, C7 Sites and the Abstraction of H4 Atom from 5-caCytN3⁺ Both in the Gas and Aqueous Phases

Table S8 The NPA Charge on O of $\bullet\text{OH}$ for Path R4 in the Gas (a) and Aqueous Phases (b)

Captions:

Fig. S1. Optimized structures of protonated 5-caCyt isomers in the aqueous phase are at CBS-QB3 approach.

Fig.S2 Optimized structures of 5-caCyt isomers in the aqueous phase are at CBS-QB3 approach.

Fig.S3 The potential energy surface (ΔG^{\ddagger} in $\text{kJ}\cdot\text{mol}^{-1}$) along the addition of $\bullet\text{OH}$ to C2, N3, C4, C7 sites of 5-caCyt in the gas phase. R^d denotes 5-caCyt+ $\bullet\text{OH}$.

Fig.S4 The potential energy surface (ΔG^{\ddagger} in $\text{kJ}\cdot\text{mol}^{-1}$) along the addition of $\bullet\text{OH}$ to C2, C4, C7 sites and the abstraction H4 atom of 5-caCytN3⁺ in the gas phase. R'^d denotes 5-caCytN3⁺+ $\bullet\text{OH}$

Fig.S5 Optimized structures of the H-bonded and π -bonded complexes for the reaction of $\bullet\text{OH}$ -mediated 5-caCyt (bond distances in \AA) in the aqueous phase at the CBS-QB3 composite approach.

Fig.S6 Optimized structures (bond distances in \AA) in the aqueous phase for the addition of $\bullet\text{OH}$ -mediated 5-caCyt (paths R1 and R2) at the CBS-QB3 composite approach.

Fig.S7 Optimized structures (bond distances in \AA) in the aqueous phase for the H-atom abstraction of $\bullet\text{OH}$ -mediated 5-caCyt (paths R3~R6) at the CBS-QB3 composite approach.

Fig.S8 Optimized structures of the H-bonded and π -bonded complexes for the reaction of $\bullet\text{OH}$ -mediated 5-caCytN3⁺ (bond distances in \AA) in the aqueous phase at the CBS-QB3 composite approach.

Fig.S9 Optimized structures (bond distances in \AA) in the aqueous phase for the addition of $\bullet\text{OH}$ -mediated 5-caCytN3⁺ (paths R1' and R2') at the CBS-QB3 composite approach.

Fig.S10 Optimized structures (bond distances in \AA) in the aqueous phase for the H-atom abstraction of $\bullet\text{OH}$ -mediated 5-caCytN3⁺ (paths R3', R5' and R6') at the CBS-QB3 composite approach.

Fig.S11 Optimized structures of the H-bonded and π -bonded complexes for the reaction of $\bullet\text{OH}$ -mediated 5-caCytCOO⁻ (bond distances in \AA) in the aqueous phase at the CBS-QB3 composite approach.

Fig.S12 Optimized structures (bond distances in \AA) in the aqueous phase for the addition of $\bullet\text{OH}$ -mediated 5-caCytCOO⁻ (paths R1'' and R2'') at the CBS-QB3 composite approach.

Fig.S13 Optimized structures (bond distances in \AA) in the aqueous phase for the H-atom abstraction of $\bullet\text{OH}$ -mediated 5-caCytCOO⁻ (paths R3''~R5'') at the CBS-QB3 composite approach.

Table S1 The Relevant Energies Information ($\text{kJ}\cdot\text{mol}^{-1}$) of Different Protonated 5-caCyt Isomers Both in the Gas and Aqueous Phases

Species	ΔE^g	ΔG^g	ΔG^s
5-caCytN3 ⁺	0.00	0.00	0.00
5-caCyt2t ⁺	1.96	2.38	27.12
5-caCyt2c ⁺	35.94	35.00	42.05
5-caCyt23t ⁺	127.68	125.36	116.45
5-caCyt23c ⁺	133.42	130.25	117.43
5-caCytN4 ⁺	104.44	102.97	87.45

At a lower pH region, there are three plausible protonation sites for 5-caCyt, namely, N3, O2, and N4, respectively. There are six isomers with respect to the protonation sites and the orientation of C2-OH group in 5-caCyt, denoted as 5-caCytN3⁺, 5-caCyt2t⁺, 5-caCyt2c⁺, 5-caCytN4⁺, 5-caCyt23t⁺, and 5-caCyt23c⁺, respectively. The order of stability obtained both in the gas and aqueous phases is 5-caCytN3⁺>5-caCyt2t⁺> 5-caCyt2c⁺>5-caCytN4⁺>5-caCyt23t⁺>5-caCyt23c⁺, and the isomer of 5-caCytN3⁺ is the most stable. Thus the reaction of •OH mediated 5-caCytN3⁺ have been reported in this study.

Table S2 The Comparison of the $\Delta G^{g\ddagger}$ (kJ·mol⁻¹) of OH Addition to C5 and C6 Sites of 5-caCyt Refined by the CBS-QB3 and G3B3 Composite Approaches

System	$\Delta G^{g\ddagger}$	
	CBS-QB3	G3B3
path R1		
IM1→P1	2.64	9.71
path R2		
IM2→P2	8.12	11.10

Table S3 Spin Contamination ($\langle S^2 \rangle$) and After Spin Annihilation ($\langle S_a^2 \rangle$) Values in •OH-mediated 5-caCyt, 5-caCytN3⁺ and 5-CytCOO⁻ Reactions

Species	$\langle S^2 \rangle^a$	$\langle S_a^2 \rangle^a$	$\langle S^2 \rangle^b$	$\langle S_a^2 \rangle^b$
•OH-mediated 5-caCyt reactions				
•OH	0.7518	0.7500	0.7518	0.7500
5-caCyt	0.0000	0.0000	0.0000	0.0000
IM1	0.7542	0.7500	0.7538	0.7500
IM2	0.7543	0.7500	0.7536	0.7500
IM3	0.7520	0.7500	0.7521	0.7500
IM4	0.7520	0.7500	0.7517	0.7500
IM5	0.7521	0.7500	0.7520	0.7500
IM6	0.7522	0.7500	0.7522	0.7500
TS1	0.7669	0.7501	0.7644	0.7501
TS2	0.7643	0.7501	0.7641	0.7501
TS3	0.7576	0.7500	0.7578	0.7500
TS4	0.7590	0.7501	0.7589	0.7501
TS5	0.7568	0.7500	0.7570	0.7500

TS6	0.7554	0.7500	0.7553	0.7500
P1	0.7558	0.7500	0.7558	0.7500
P2	0.7657	0.7502	0.7602	0.7501
P3	0.7575	0.7500	0.7712	0.7502
P4	0.7673	0.7501	0.7661	0.7501
P5	0.7556	0.7500	0.7551	0.7500
P6	0.7564	0.7500	0.7592	0.7501
•OH-mediated 5-caCytN3 ⁺ reactions				
5-caCytN3 ⁺	0.0000	0.0000	0.0000	0.0000
IM1'	0.7519	0.7500	0.7526	0.7500
IM2'	0.7522	0.7500	0.7521	0.7500
IM3'	0.7522	0.7500	0.7522	0.7500
IM4'	0.7521	0.7500	0.7521	0.7500
IM5'	0.7522	0.7500	0.7524	0.7500
IM6'	0.7522	0.7500	0.7522	0.7500
TS1'	0.7698	0.7501	0.7674	0.7501
TS2'	0.7630	0.7501	0.7636	0.7501
TS3'	0.7574	0.7500	0.7578	0.7500
TS4'	0.7553	0.7500	0.7562	0.7500
TS5'	0.7576	0.7500	0.7576	0.7500
TS6'	0.7550	0.7500	0.7554	0.7500
P1'	0.7568	0.7500	0.7566	0.7500
P2'	0.7567	0.7500	0.7569	0.7500
P3'	0.7610	0.7501	0.7705	0.7502
P4'	0.7558	0.7500	0.7577	0.7500
P5'	0.7555	0.7500	0.7555	0.7500
P6'	0.7557	0.7500	0.7555	0.7500
•OH-mediated 5-CytCOO ⁻ reactions				
5-CytCOO ⁻	0.0000	0.0000	0.0000	0.0000
IM1''	0.7521	0.7500	0.7520	0.7500
IM2''	0.7521	0.7500	0.7518	0.7500
IM3''	0.7521	0.7500	0.7518	0.7500
IM4''	0.7517	0.7500	0.7517	0.7500
IM5''	0.7521	0.7500	0.7573	0.7500
TS1''	0.7653	0.7501	0.7637	0.7501
TS2''	0.7656	0.7501	0.7643	0.7501
TS3''	0.7573	0.7500	0.7577	0.7500
TS4''	0.7575	0.7500	0.7581	0.7500
TS5''	0.7573	0.7500	0.7573	0.7500
P1''	0.7559	0.7500	0.7562	0.7500
P2''	0.7573	0.7500	0.7566	0.7500
P3''	0.7681	0.7502	0.7682	0.7502
P4''	0.7596	0.7500	0.7590	0.7500
P5''	0.7568	0.7500	0.7564	0.7500

^a at the B3LYP/6-311G(2d,d,p); ^b at the PCM//B3LYP/6-311G(2d,d,p) level

Table S4 The Relevant Energies Information (kJ·mol⁻¹) of Different 5-caCyt Isomers Both in the Gas and Aqueous Phases

Species	ΔE^g	ΔG^g	ΔG^s
---------	--------------	--------------	--------------

M1	0.00	0.00	0.00
M2	11.04	10.01	7.62

Table S5 The Energy Information ^a (kJ·mol⁻¹) for the Addition of •OH to C2, N3, C4, C7 Sites of 5-caCyt Both in the Gas and Aqueous Phases

System	CBS-QB3 ^b				PCM ^c			
	ΔE^g	$\Delta E^{g\ddagger}$	ΔG^g	$\Delta G^{g\ddagger}$	ΔE^s	$\Delta E^{s\ddagger}$	ΔG^s	$\Delta G^{s\ddagger}$
R ^d	0.00		0.00		0.00		0.00	
C2-IM	-24.19		9.72		-5.57		28.41	
C2-TS	34.32		74.97		54.79		95.24	
C2-P	-9.43		31.73		15.57		56.23	
N3-IM	-24.98		7.55		-9.03		23.56	
N3-TS	37.70		77.48		63.80		102.95	
N3-P	17.50		54.91		52.91		89.02	
C4-IM	-24.96		7.57		-9.03		23.56	
C4-TS	20.15		61.53		36.82		77.76	
C4-P	-12.02		26.84		7.76		46.19	
C7-IM	-14.29		14.35		-10.13		16.22	
C7-TS	48.81		88.23		52.22		92.09	
C7-P	-3.80		35.52		5.58		45.58	
C2-IM→C2-P		58.51		65.25		60.36		66.83
N3-IM→N3-P		62.68		69.93		72.83		79.39
C4-IM→C4-P		45.11		53.96		45.85		54.20
C7-IM→C7-P		63.10		73.88		62.35		75.87

^a ΔE^g , $\Delta E^{g\ddagger}$, ΔG^g , and $\Delta G^{g\ddagger}$ are relative energy, activation energy, relative free energy, and activation free energy in the gas phase, respectively; ΔE^s , $\Delta E^{s\ddagger}$, ΔG^s , and $\Delta G^{s\ddagger}$ are relative energy, activation energy, relative free energy, and activation free energy with PCM model based on the optimized geometries in the aqueous phase. ^b CBS-QB3 composite approach. ^c CBS-QB3 with PCM model. ^d denotes 5-caCyt+•OH.

Table S6 The Nucleus-independent Chemical Shifts (NICS(0)) for the Product Radicals of •OH Abstraction from 5-caCyt in the Gas Phase

	P3	P4	P5	P6
NICS(0)	-0.64	-2.16	-5.82	-0.04

Table S7 The Energy Information ^a (kJ·mol⁻¹) for the Addition of •OH to C2, C4, C7 Sites and the Abstraction of H4 Atom from 5-caCytN3⁺ Both in the Gas and Aqueous Phases

System	CBS-QB3 ^b	PCM ^c
--------	----------------------	------------------

	ΔE^g	$\Delta E^{g\ddagger}$	ΔG^g	$\Delta G^{g\ddagger}$	ΔE^s	$\Delta E^{s\ddagger}$	ΔG^s	$\Delta G^{s\ddagger}$
R' ^d	0.00		0.00		0.00		0.00	
C2-IM'	-27.83		-2.44		-5.55		18.06	
C2-TS'	36.13		76.37		57.36		98.29	
C2-P'	-5.52		33.18		19.78		58.40	
C4-IM'	-27.85		-2.40		-5.56		17.74	
C4-TS'	40.62		80.63		57.62		98.51	
C4-P'	1.63		39.09		15.24		54.20	
C7-IM'	-27.85		-2.40		-5.56		17.74	
C7-TS'	33.10		73.26		50.53		90.99	
C7-P'	-2.33		-35.99		10.05		49.94	
H4-IM'	-22.16		4.20		-3.81		20.95	
H4-TS'	63.69		96.98		84.08		118.8	
H4-P'	16.22		50.92		26.07		60.28	
C2-IM'→C2-P'		63.96		78.81		62.91		80.23
C4-IM'→C4-P'		68.47		83.03		63.18		80.77
C7-IM'→C7-P'		60.95		75.66		56.09		73.25
H4-IM'→H4-P'		85.85		92.77		87.89		97.90

^a ΔE^g , $\Delta E^{g\ddagger}$, ΔG^g , and $\Delta G^{g\ddagger}$ are relative energy, activation energy, relative free energy, and activation free energy in the gas phase, respectively; ΔE^s , $\Delta E^{s\ddagger}$, ΔG^s , and $\Delta G^{s\ddagger}$ are relative energy, activation energy, relative free energy, and activation free energy with PCM model based on the optimized geometries in the aqueous phase. ^b CBS-QB3 composite approach. ^c CBS-QB3 with PCM model. ^d denotes 5-CaCytN3⁺ +•OH.

Table S8 The NPA Charge (e) on O of •OH for Path R4 in the Gas (a) and Aqueous Phases (b)

	a	b
ρ_o	0.287	-0.415

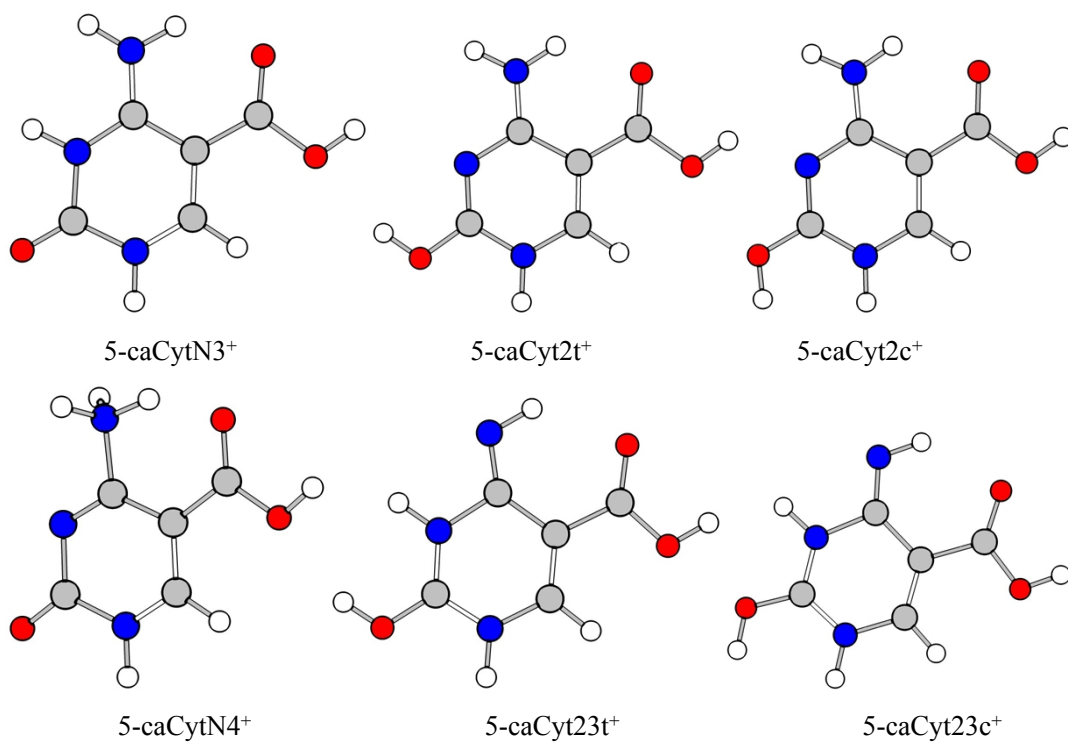


Fig. S1

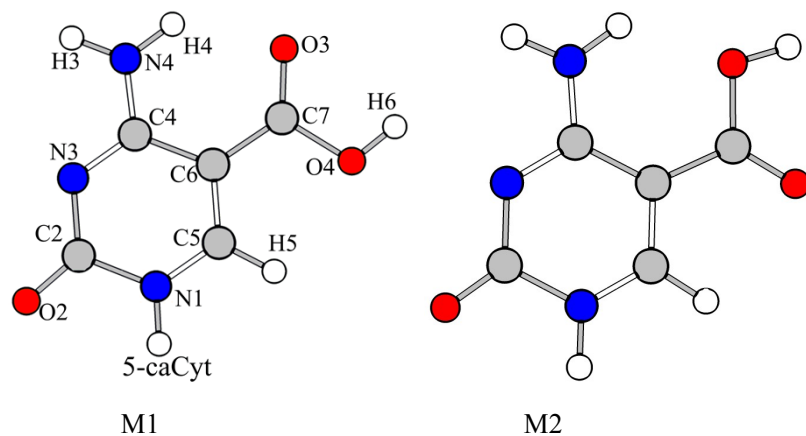


Fig. S2

The dihedral angles $\tau(\text{C2-N3-C4-C5})$, $\tau(\text{N3-C4-C5-C6})$, $\tau(\text{C4-C5-C6-N1})$, and $\tau(\text{C5-C6-N1-C2})$ are all 0.0° for the pyrimidine ring of 5-caCyt, suggesting a planar geometry and the ring π -system. The corresponding dihedral angles $\tau(\text{O2-C2-N3-C4})$, $\tau(\text{H3-N4-C4-C5})$, $\tau(\text{H4-N4-C4-C5})$, $\tau(\text{O3-C7-C5-C6})$, and $\tau(\text{O4-C7-C5-C6})$ are also 0.0° for 5-caCyt, implying that the more planar character is found in C=O, -NH₂, and -COOH of 5-caCyt, respectively. The constituent atoms of these bonds are expected to be more reactive for the electrophilic addition reaction with hydroxyl radical. The structural features of 5-caCyt are favored C2, O2, N3, C4, C5, C6, C7, and O3 as the addition sites.

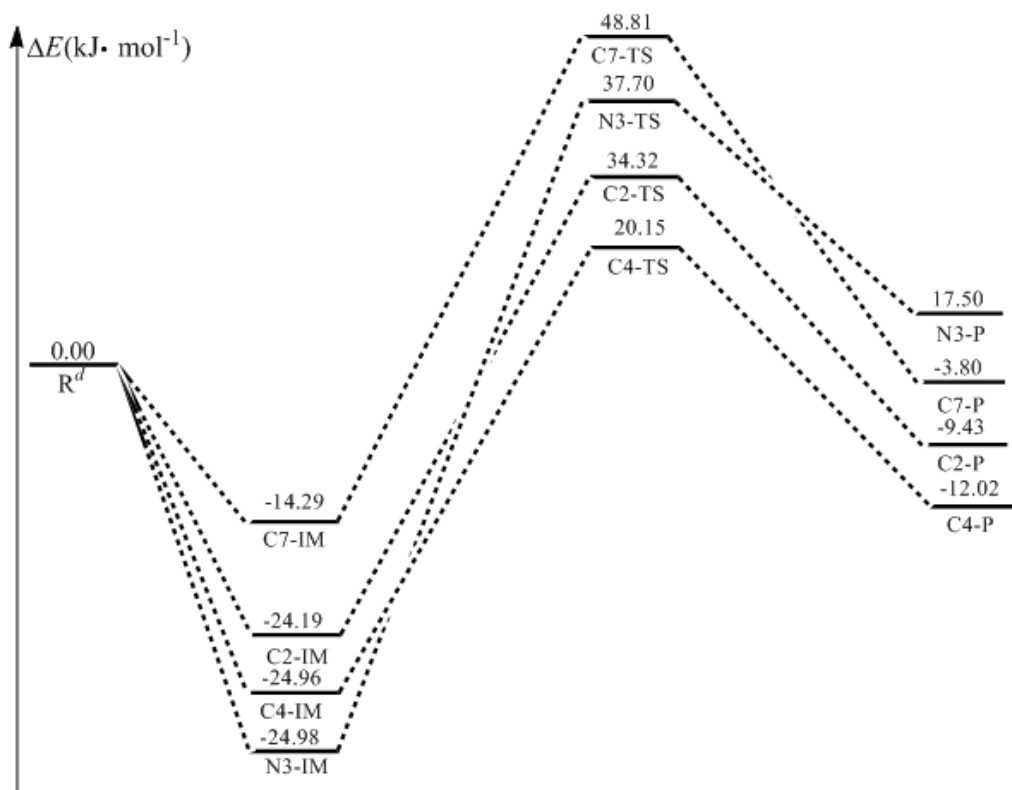


Fig.S3

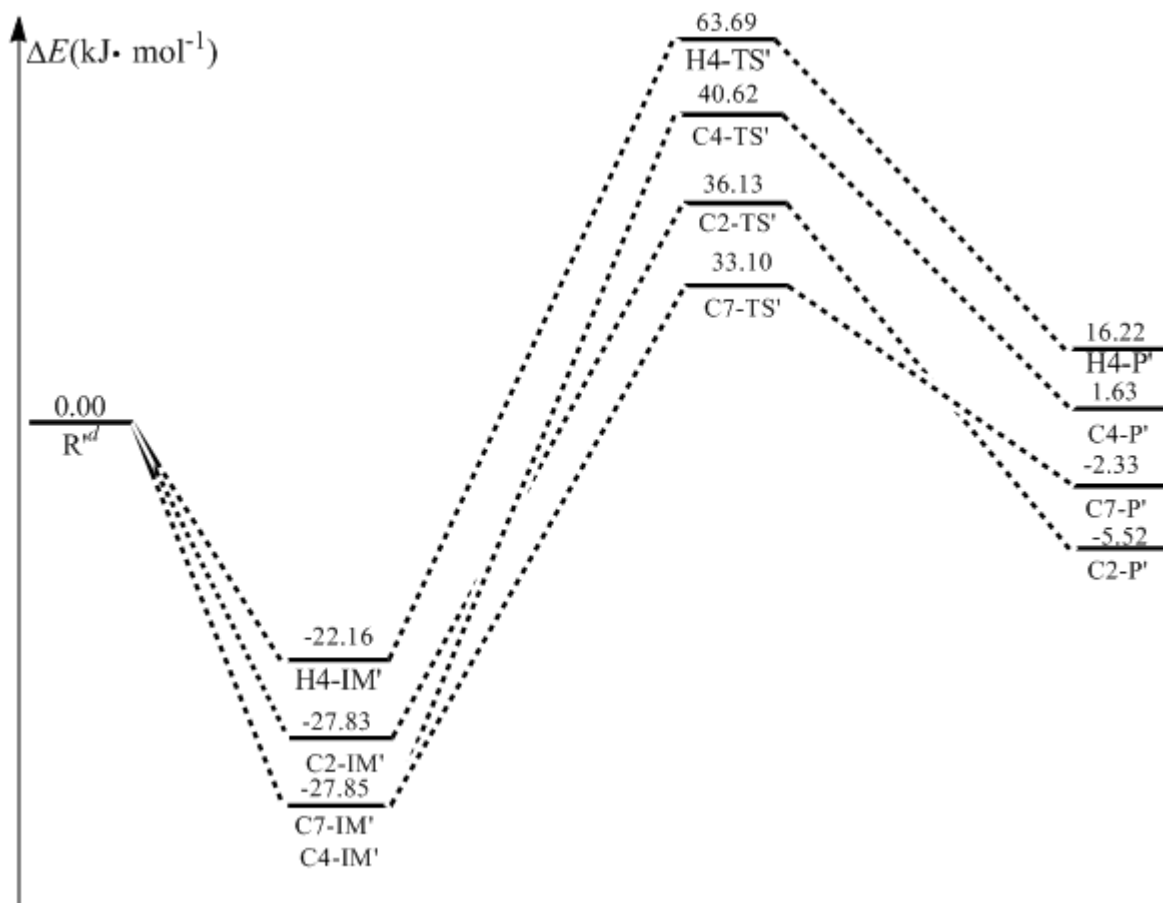


Fig.S4

As for the $\bullet\text{OH}$ addition to C2, C4, C5, C6 and C7 sites of 5-caCytN3^+ , the ΔE^{\ddagger} between the initial reactants and the TSs are 63.96, 68.47, 23.12, 36.46, and 60.95 $\text{kJ}\cdot\text{mol}^{-1}$, respectively, suggesting that the $\bullet\text{OH}$ addition to C5 and C6 sites are more favorable kinetically than to other sites. Moreover, $\bullet\text{OH}$ addition to C5 and C6 sites are strong exothermic with respect to their energy of the reaction complexes, whereas the reactions of other sites are endothermic with respect to their energy of the reaction intermediates. These results imply that the addition of $\bullet\text{OH}$ to 5-caCytN3^+ at C2, C4 and C7 sites are both thermodynamically and kinetically less favorable than addition to C5 and C6 sites. The same case exists in the H4 atom abstraction of 5-caCytN3^+ .

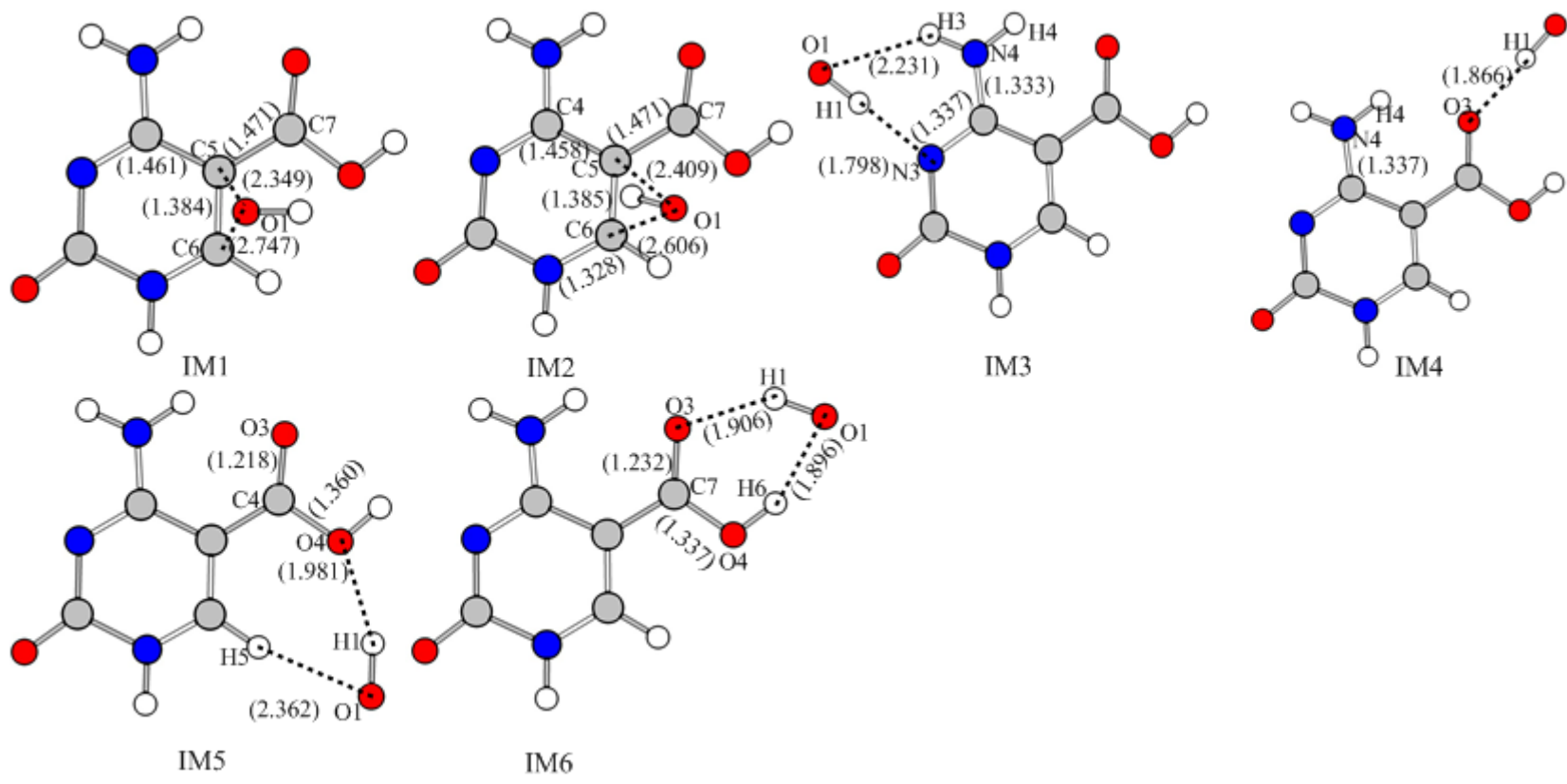


Fig. S5

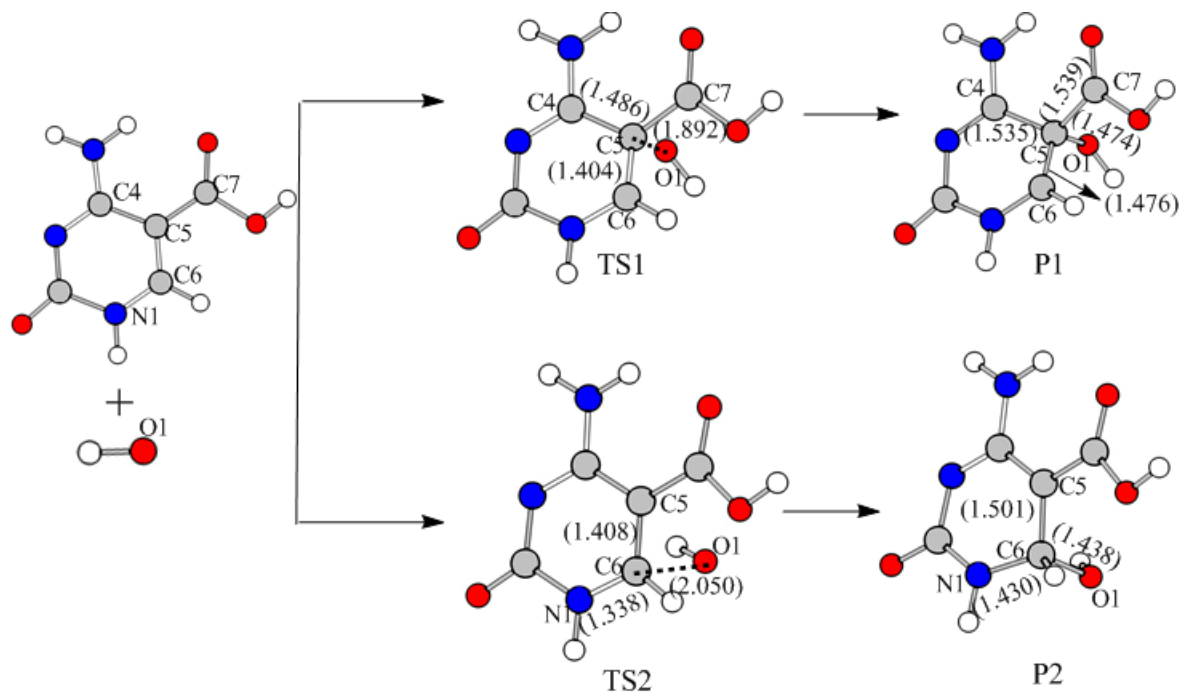


Fig. S6

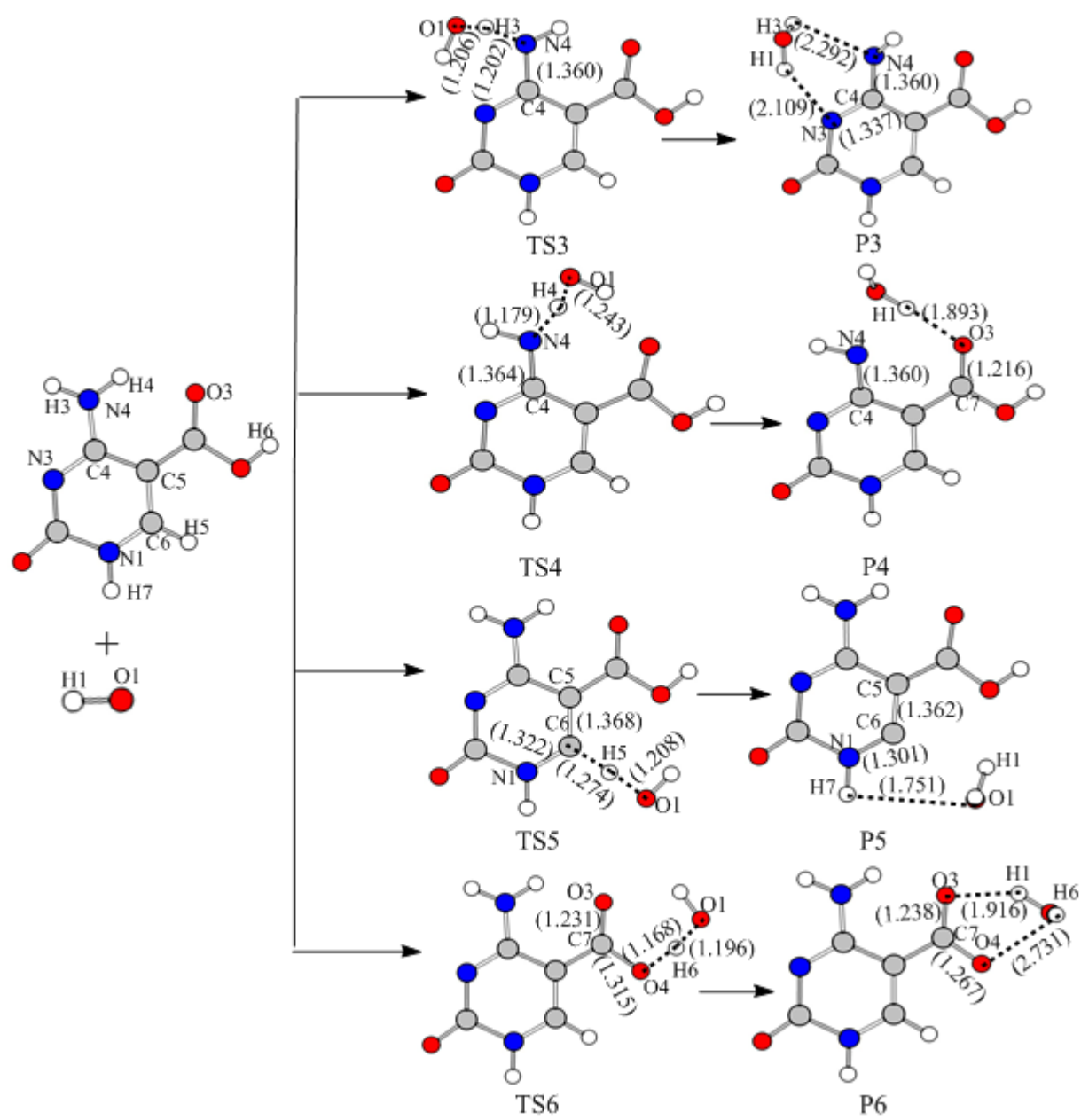


Fig. S7

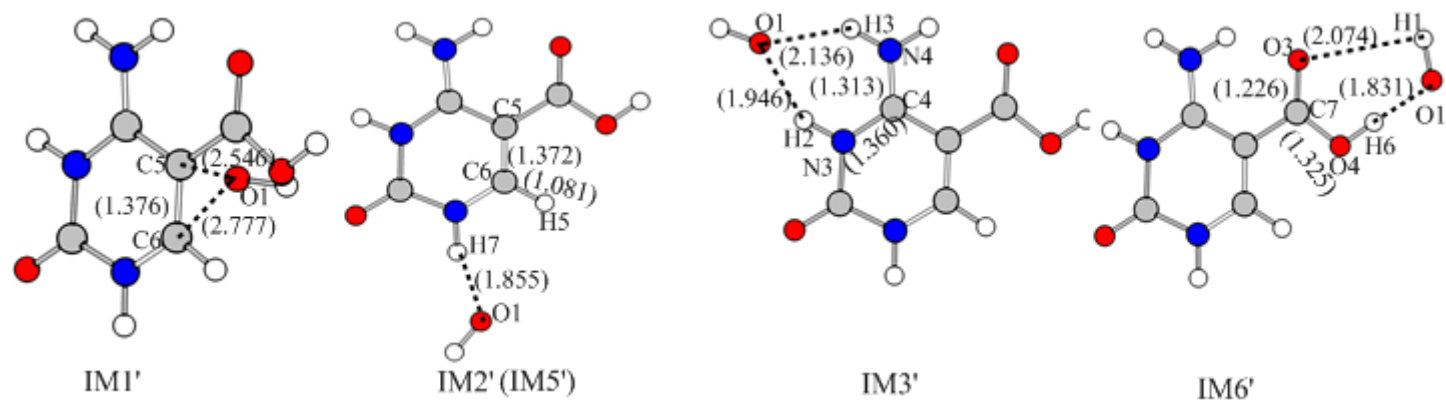


Fig. S8

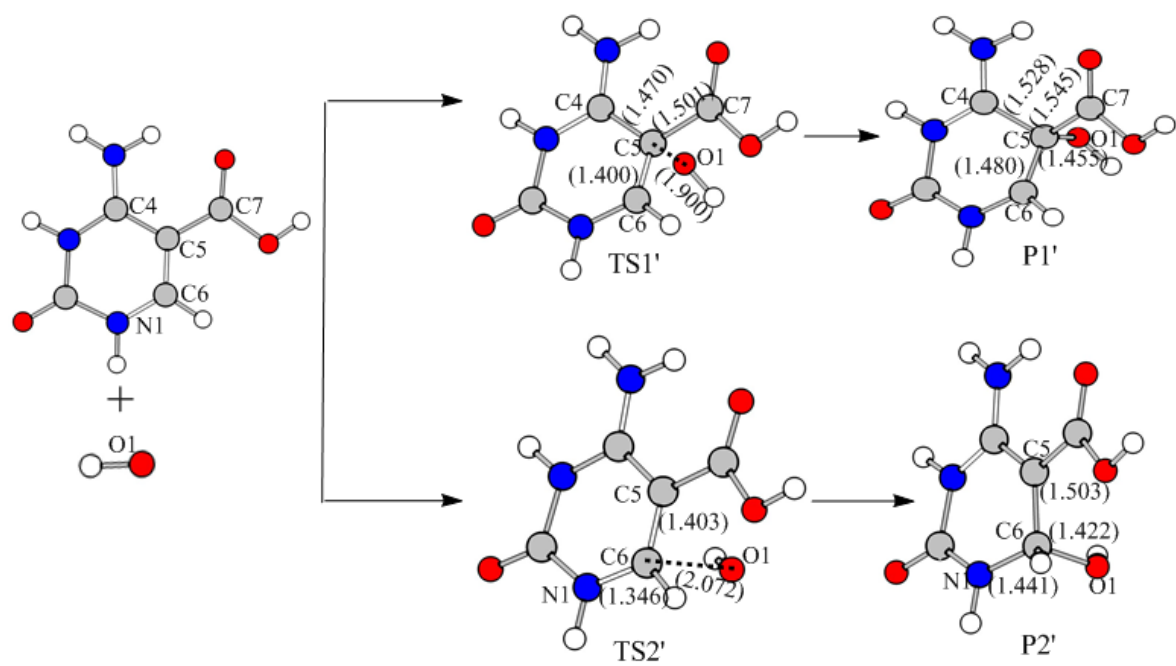


Fig. S9

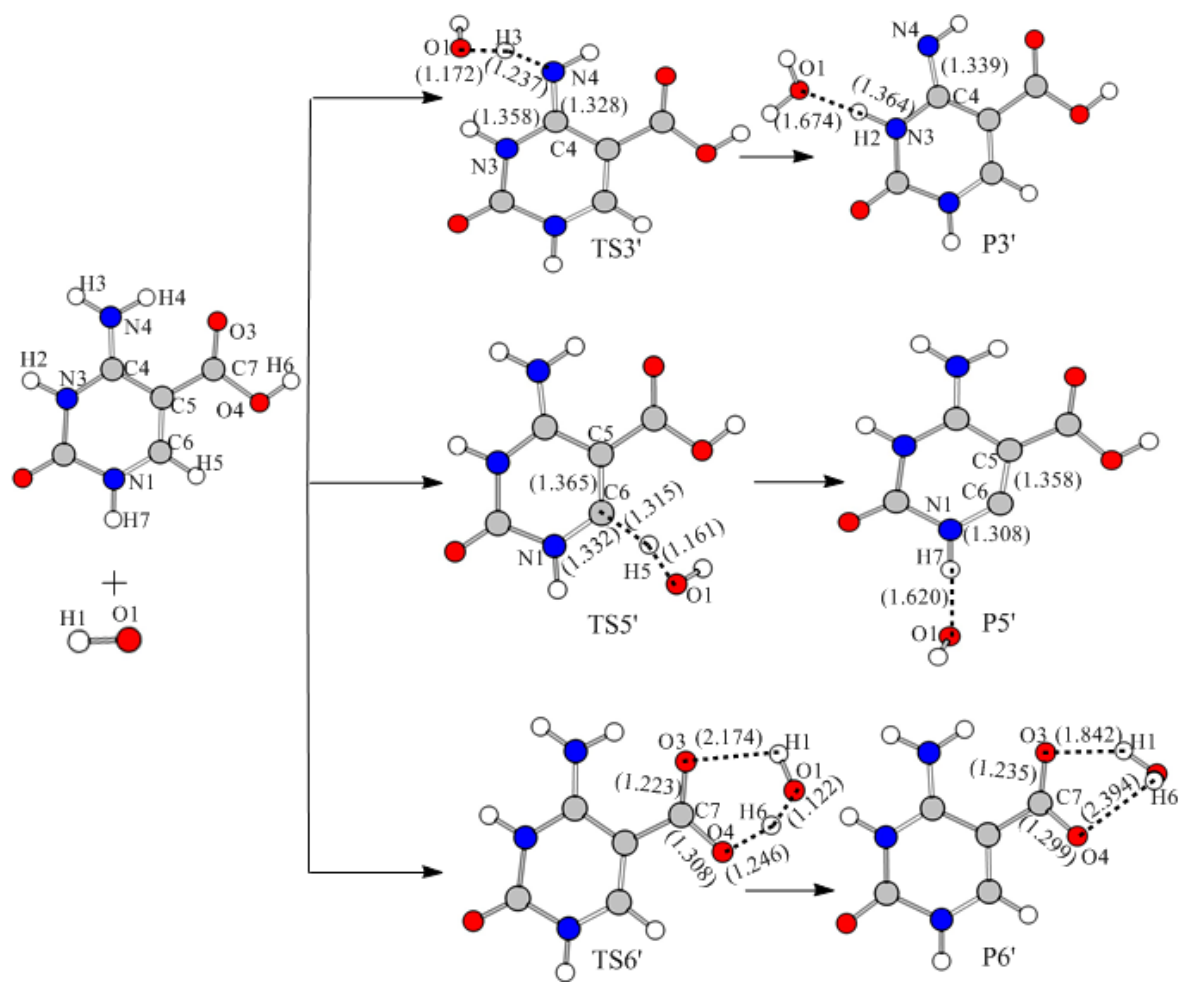


Fig. S10

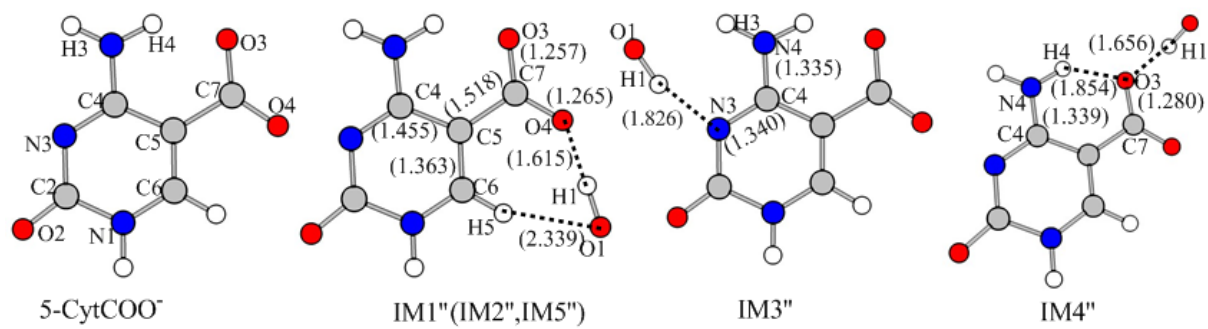


Fig. S11

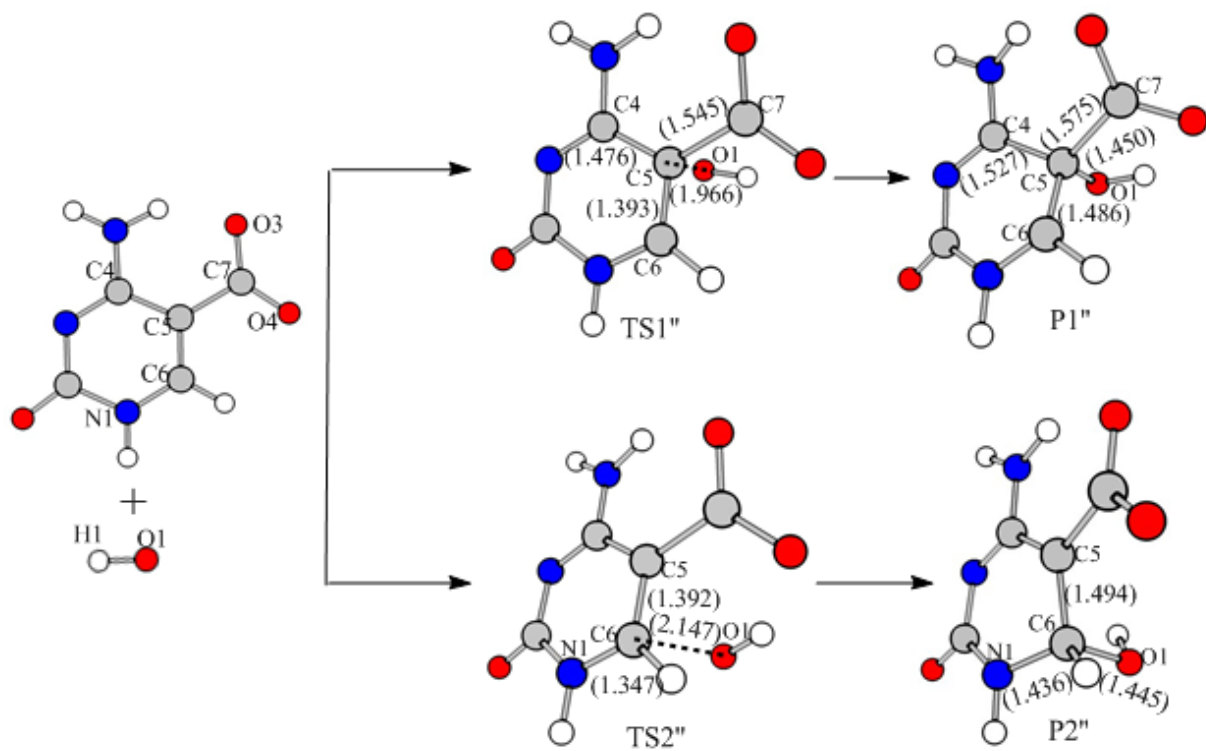


Fig. S12

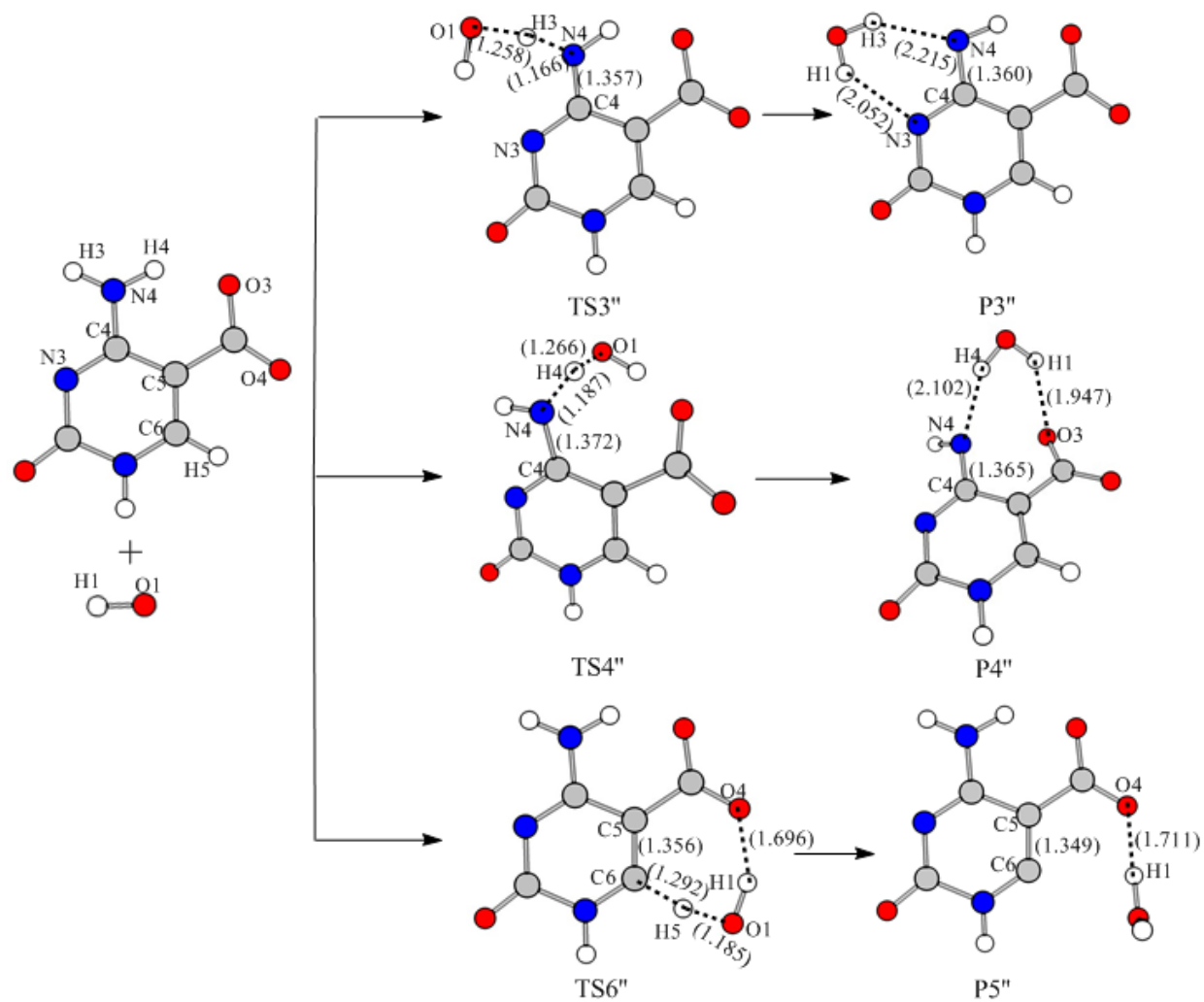


Fig. S13